LETTERS

Aberrant innate immune response in lethal infection of macaques with the 1918 influenza virus

Darwyn Kobasa[1], Steven M. Jones[2,3], Kyoko Shinya[5], John C. Kash[6], John Copps[8], Hideki Ebihara[2,9,10,11], Yasuko Hatta[12], Jin Hyun Kim[12], Peter Halfmann[12], Masato Hatta[12], Friederike Feldmann[2], Judie B. Alimonti[2], Lisa Fernando[2], Yan Li[1], Michael G. Katze[6,7], Heinz Feldmann[2,4] & Yoshihiro Kawaoka[9,10,11,12]

The 1918 influenza pandemic was unusually severe, resulting in about 50 million deaths worldwide[1]. The 1918 virus is also highly pathogenic in mice, and studies have identified a multigenic origin of this virulent phenotype in mice[2–4]. However, these initial characterizations of the 1918 virus did not address the question of its pathogenic potential in primates. Here we demonstrate that the 1918 virus caused a highly pathogenic respiratory infection in a cynomolgus macaque model that culminated in acute respiratory distress and a fatal outcome. Furthermore, infected animals mounted an immune response, characterized by dysregulation of the antiviral response, that was insufficient for protection, indicating that atypical host innate immune responses may contribute to lethality. The ability of influenza viruses to modulate host immune responses, such as that demonstrated for the avian H5N1 influenza viruses[5], may be a feature shared by the virulent influenza viruses.

Genes of the 1918 virus were constructed from published sequences[6–11], and the virus was generated using plasmid-based reverse genetics, as previously described[12]. The virus was highly virulent in intranasally inoculated mice with an LD_{50} (dose required to kill 50% of animals) of $10^{3.5}$ plaque-forming units (PFU), comparable to that previously reported[4]. Cynomolgus macaques (*Macaca fascicularis*), previously used to study H5N1 influenza virus pathogenesis[13,14], were selected as a nonhuman primate model for further analysis of virulence. Macaques ($n = 7$) were infected with the 1918 virus) or a conventional human virus, A/Kawasaki/173/01 (K173; H1N1) ($n = 3$), via multiple routes, as in the H5N1 virus experiment[13]. All 1918-virus-infected animals became symptomatic within 24 h post-infection. They appeared depressed, were hesitant to eat or drink normal food items, and showed respiratory complications such as nasal discharge and non-productive cough. They became progressively more debilitated and eventually developed an acute respiratory distress syndrome. Two macaques infected with the 1918 virus and one with K173 were euthanized on each of days 3 and 6 for analysis. Of these, one 1918-virus-infected animal had reached the predetermined score for euthanasia on day 6. The remaining animals, originally scheduled for euthanasia on day 21 post-infection, were euthanized on day 8 owing to severity of symptoms in 1918-virus-infected animals.

In 1918-virus-infected animals respiratory signs were the most pronounced indication of illness with an increase in respiration rate, from a post-infection average of 26.4, to a range of 72–84 on day 8. Decreases in lung function shown by a decrease in blood oxygen saturation of as much as 36% compared with pre-infection levels were detected by pulse oximetry. Consistent changes in heart rate and blood pressure were not observed. In contrast, animals infected with the K173 virus showed few, very mild, clinical signs.

The 1918 virus was present at high titres in both the upper and lower respiratory tissues on days 3, 6 and 8, whereas the K173 virus was isolated mainly from the upper respiratory tissues on days 3 and 6 at appreciably lower titres and on day 8 in only one tonsil (Fig. 1). The 1918 virus was recovered from the heart and spleen of some animals, but neither virus was isolated from the brain, kidneys, liver or colon of any animal. Virus was detected more efficiently with nasal or throat swabs from 1918-virus-infected animals than for K173-virus-infected animals (Supplementary Table 1), but neither virus was isolated in rectal or genital swabs, or in the blood, on any day.

Lungs of the 1918-virus-infected macaques were the only tissue to exhibit macroscopic pathologic changes as severe lesions, with 60% to 90% of the lung tissue affected by days 6–8 (Supplementary Fig. 1). Profuse watery and bloody liquid filled infected areas, greatly reducing lung function. On day 3 with either virus, there was evidence of some degree of alveolar damage with concomitant detection of viral antigen (Supplementary Fig. 2a–i); however, K173 was not isolated from the lungs, indicating low levels of replication. In contrast to lesions of the K173-infected animal, lungs of 1918-virus-infected animals showed infection of multifarious cells of the alveolar wall on day 3 (Supplementary Fig. 2f, g). Common to infection with either the K173 or 1918 virus were flattened linear alveolar cells that were positive for viral antigen without showing desquamation into the alveolar space (Supplementary Fig. 2d, f). A prominent characteristic of 1918-virus-infected lungs was antigen in plump alveolar cells and desquamation of these cells into the alveolar space (Supplementary Fig. 2g, h). These differences in the early phase of infection between the 1918 and K173 viruses might account for later differences in inflammation and the eventual pathologic state of the lungs.

By days 6 and 8, the lungs of K173-virus-infected animals showed signs of healing, evidenced by thickening of the alveolar wall and no viral antigen expression (Fig. 2a–c, day 8; day 6 not shown). In contrast, the lungs of all 1918-virus-infected animals showed worsening alveolar damage and substantial viral antigen (Fig. 2d–h). Extensive oedema and haemorrhagic exudates were prominent (Fig. 2d–f), as reported for patients who succumbed to the 'Spanish' influenza[15]. By day 8, expression of viral antigen was diminished

[1]Respiratory Viruses, and [2]Special Pathogens Program National Microbiology Laboratory, Public Health Agency of Canada, Winnipeg, Manitoba R3E 3R2, Canada. [3]Department of Immunology and [4]Department of Medical Microbiology, University of Manitoba, Winnipeg, Manitoba R3E 3R2, Canada. [5]The Avian Zoonosis Research Centre, Tottori University, Tottori 680-8550, Japan. [6]Department of Microbiology, School of Medicine, and [7]Washington National Primate Research Center, University of Washington, Seattle, Washington 98195, USA. [8]National Centre for Foreign Animal Diseases, Canadian Food Inspection Agency, Canadian Science Centre for Human and Animal Health, Winnipeg, Manitoba R3E 3M4, Canada. [9]Division of Virology, Department of Microbiology and Immunology and [10]International Research Center for Infectious Diseases, Institute of Medical Science, University of Tokyo, Tokyo 108-8639, Japan. [11]CREST, Japan Science and Technology Agency, Saitama 322-0012, Japan. [12]Department of Pathobiological Sciences, University of Wisconsin-Madison, Madison, Wisconsin 53706, USA.

©2007 Nature Publishing Group

or undetectable in consolidated alveolar areas, but still appreciable around consolidated areas (Fig. 2g). Bronchiolitis and bronchitis with expression of viral antigen were prominent at this time (Fig. 2h).

Among the chemokines and cytokines tested (see Methods), substantial increases of interleukin-6 (IL-6), IL-8, CCL2 (monocyte chemotactic protein-1) and CCL5 (RANTES) were detected in the sera of infected animals compared with pre-infection levels. No changes in IL-2, IL-4, IFNγ or TNF-α were detected. Both IL-8 (day 6) and CCL5 (days 6 and 8) were elevated to similar levels in animals infected with either virus (Fig. 3). CCL2 was elevated 1.4- to 1.8-fold in K173-infected animals on days 3 and 6, respectively, whereas in the 1918-virus-infected animals, increases were higher (2- to 4-fold), but did not achieve statistical significance. The most striking changes were seen in IL-6. On day 0, IL-6 in all macaques ranged from 2.85 to 13.04 pg ml^{-1}, except for one animal with a baseline measurement of 251.32 pg ml^{-1}. In 1918-virus-infected animals, IL-6 increased 3- to 9-fold by day 3 post-infection ($P = 0.10$), 6- to 19-fold by day 6 ($P = 0.07$), and 5- to 25-fold by day 8, while remaining throughout the study between 2.85 and 4.59 pg ml^{-1} in the K173-infected animals. In humans experimentally infected with influenza virus, IL-6

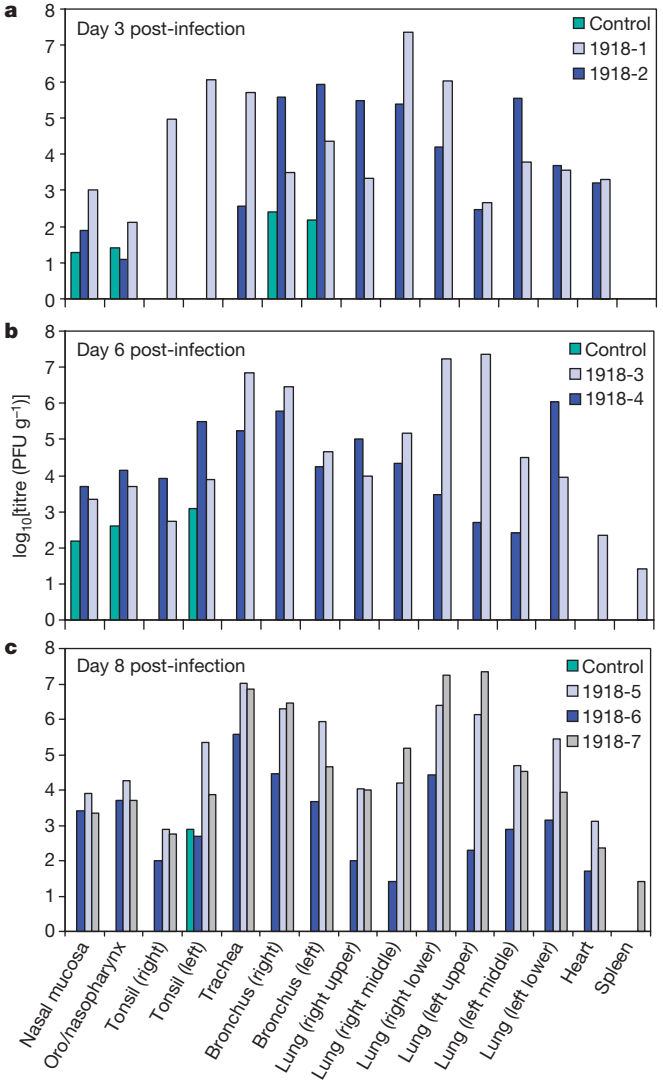

Figure 1 | Viral replication in nonhuman primate tissues. **a**–**c**, Virus titres were determined in plaque assays of tissue homogenates on days 3 (**a**), 6 (**b**) and 8 (**c**) post-infection in animals infected with the K173 (control) or 1918 virus (1918-1 to 1918-7). Individual titres for each tissue in each animal are reported as $\log_{10}$ (PFU per g tissue). Virus was not isolated from the colon, liver, kidneys or brain of any animal.

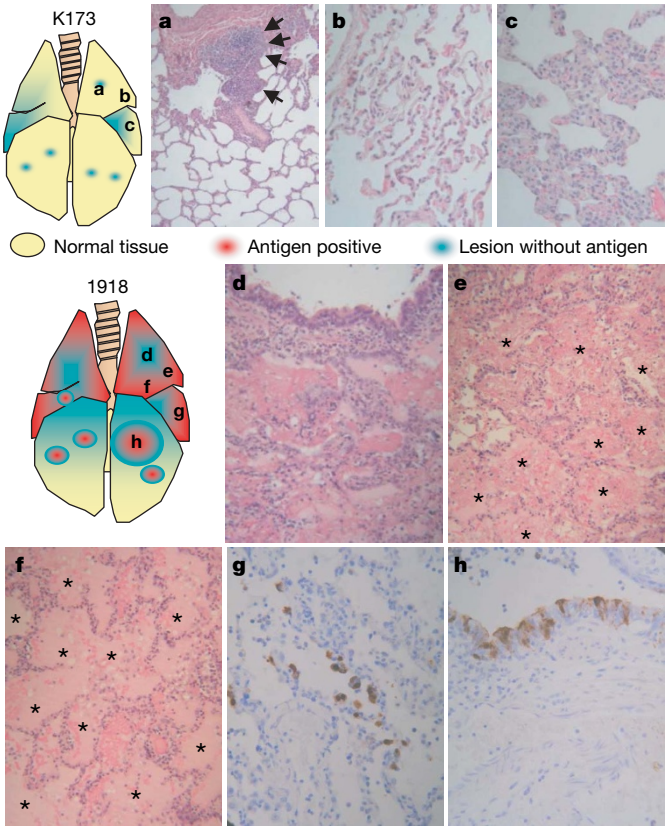

Figure 2 | Pathologic examination of lungs infected with the 1918 or K173 virus on day 8 post-infection. **a**, In lungs of a K173-virus-infected animal, peribronchiolitis with lymph follicle formation was detected throughout the lung (arrows). **b**, **c**, Mild thickening of the alveolar wall was observed in the middle lobes, but antigen was not detected. **d**–**f**, Most areas of the lungs of a 1918-virus-infected animal contained consolidated lesions (**d**) consisting of bronchiolitis and alveolitis (**e**) with fibrinous and inflammatory exudates (*) and alveolar oedema (**f**) with proteinaceous fluid and haemorrhage (*). **g**, **h**, Viral antigen (brown) was detected in the large regenerative alveolar cells (**g**) and the bronchiolar epithelial cells in lesions (**h**). Magnifications are ×25 in **a**; ×240 in **b**, **c**, **g** and **h**; and ×120 in **d**–**f**.

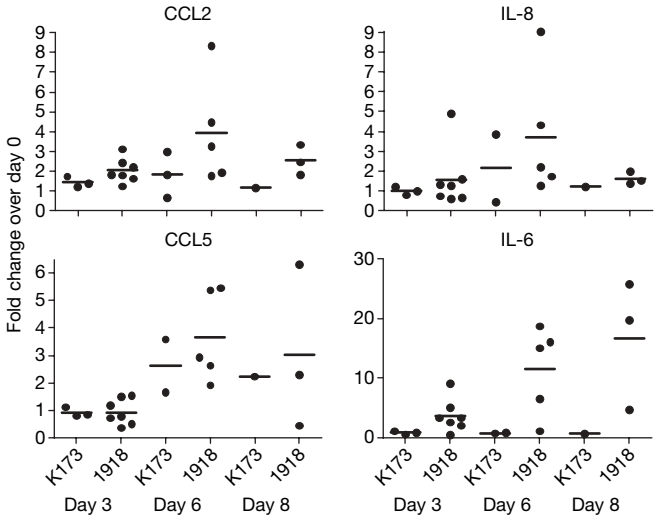

Figure 3 | Chemokine and cytokine levels in serum. The levels of chemokines (CCL2 and CCL5) and cytokines (IL-6 and IL-8) in serum were analysed by a cytometric bead array assay. The levels on days 3, 6 and 8 were compared with the day 0 baseline to determine the relative changes within each animal. The bars represent the average for each group.

©2007 Nature Publishing Group

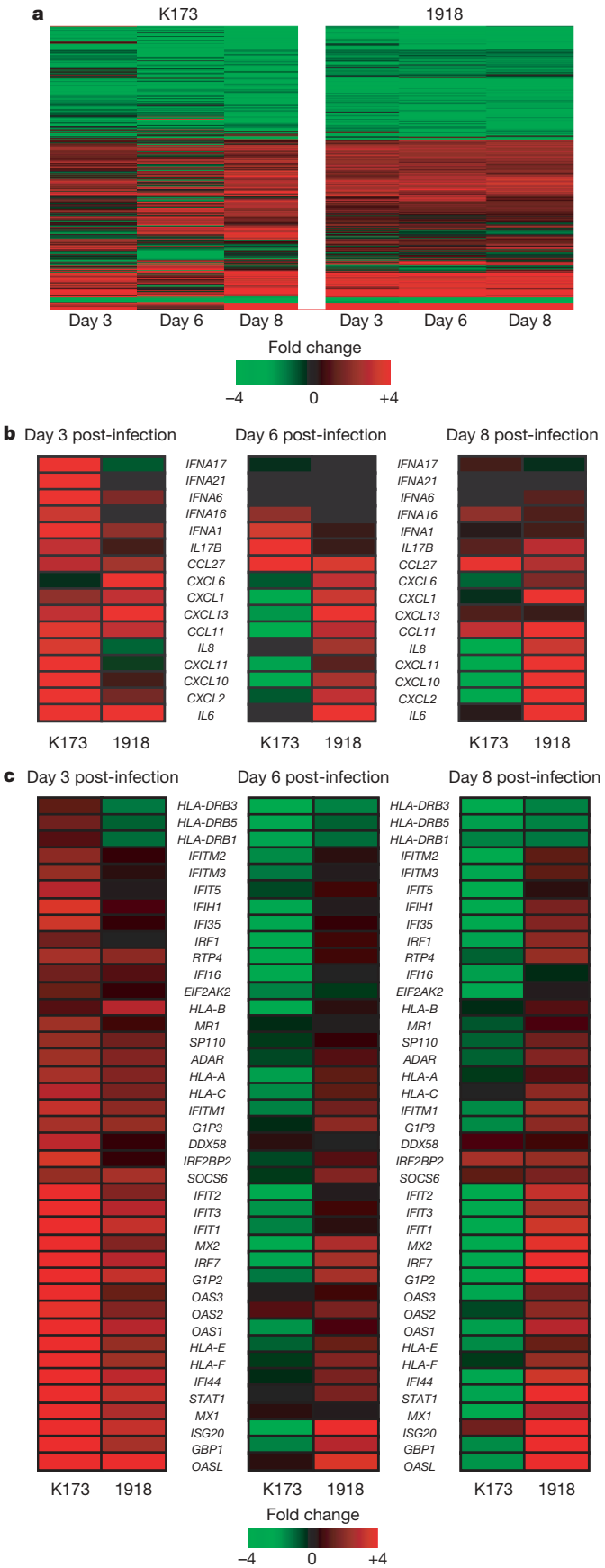

expression at both the site of replication and in sera directly correlated with the extent of viral shedding and fever and is thought to have a role in mediating the clinical manifestations of infection[16,17]. A similar relationship may also explain the progression to severe clinical signs in macaques infected with the 1918 virus.

To investigate the regulation of the host response to the 1918 virus, we considered the global gene expression profiles in bronchi, a lower respiratory tissue with substantial replication of both viruses (see Fig. 1a–c), using microarray analysis (Fig. 4a, b). In general, overall gene expression patterns of individual 1918-virus-infected animals were similar, particularly on days 6–8 (Supplementary Fig. 3). One striking observation was the relative constancy in gene expression profiles in the 1918-virus-infected animals at days 3 through 8 post-infection, in marked contrast to the K173 virus-infected animals, which showed an appreciably more dynamic response during the course of infection. The sustained host response in 1918-virus-infected macaques is similar to that recently reported in 1918-virus-infected mice[18], indicating that critical decisions influencing the outcome of the infection may occur very early, as recently suggested for H5N1 virus infection in humans[19]. The functional response associated with the observed gene expression changes was analysed by gene ontology (see Methods). This analysis demonstrated that activation of immune-response-related genes in K173-infected animals was highest at day 3 post-infection, whereas the expression of these genes was relatively constant throughout the course of 1918 virus infection (Supplementary Fig. 4). Interestingly, we observed a dramatic activation of genes involved in cellular metabolism in the K173-infected animals on days 6 to 8 post-infection, probably due to cell proliferation and tissue remodelling after clearance of the virus.

Detailed analysis of immune-response-related gene expression changes (Fig. 4b) demonstrated that bronchi from both groups of animals showed activation of several inflammatory chemokine and cytokine genes, including *CCL11* and *IL-6*. *IL-6* messenger RNA was expressed at a high level until day 8 post-infection in the 1918-virus-infected animals, but not the K173-infected animals, consistent with levels detected in serum (Fig. 3). Several key cytokine genes, including *IL-8* and *CXCL11*, showed a delay in activation in 1918-virus-infected animals, although several chemokines important for the activation and recruitment of neutrophils, including *CXCL6* and *CXCL1*, were preferentially upregulated. Strikingly, K173-infected animals showed a marked increase in expression of mRNAs for many type I interferons (IFNs) and a corresponding increase in mRNA expression of type-I-IFN-stimulated genes early in infection (Fig. 4c), coinciding with the greatest load of the virus (Fig. 1). This response was downregulated on days 6 and 8 post-infection, when the K173 virus was not detected. 1918-virus-infection, in contrast, induced much fewer IFN-α genes, suggesting that it caused an altered antiviral response in the bronchus. Accordingly, the 1918-virus-infected animals also showed differential activation of type-I-IFN-stimulated gene expression on days 3 to 8, despite viral titres in bronchi that were 10–5,000-fold higher than in K173-virus-infected

Figure 4 | Microarray analysis of gene expression in the bronchi of macaques on days 3, 6 and 8 post-infection. **a**, Overall gene expression profiles in K173- and 1918-virus-infected animals. **b**, Expression of chemokines and cytokines as determined by expression oligonucleotide microarray analysis of bronchial tissue from macaques infected with the K173 or 1918 influenza virus. **c**, Expression of type I interferon (IFN)-stimulated genes in K173- and 1918-virus-infected macaque bronchi. For each K173 virus infection point, the data presented are gene expression changes calculated from technical replicate arrays ($n = 4$). The data shown for the day 3 and day 6 1918 virus infections are error-weighted averages for two animals ($n = 8$ arrays), whereas the day 8 1918 virus infection data are the error-weighted averages for three animals ($n = 12$ arrays). Genes included in this figure showed ≥2-fold ($P < 0.01$) differences in expression in at least one experiment. Genes shown in red were upregulated and those shown in green were downregulated in infected relative to mock-infected animals. See Supplementary Table 2 for full gene names.

©2007 Nature Publishing Group

animals. Although the mechanisms underlying the differences in regulation of type I IFN responses remain elusive, our data suggest that the 1918 virus induces an antiviral response different from that of K173, possibly including reduced sensitivity to type I IFN responses. Finally, IFN-β1 mRNA was either not induced or was down-regulated in all samples except for a modest induction of IFN-β1 in the K173-infected animal at day 3 post-infection (not shown). Only limited IFN-β1 expression might be expected given that IFN-β1 is a first-wave interferon and would probably be induced earlier than our first sample collection (that is, day 3).

An important pathway in activation of the antiviral response to influenza virus infection occurs through the activities of DDX58 (or retinoic-acid-inducible protein I) and IFIH1 (or melanoma differentiation-associated gene 5)[20,21]. Both genes were induced in the K173-virus-infected, but not the 1918-virus-infected, animals (Fig. 4d). The nonstructural protein 1 (NS1) protein of virulent influenza viruses can modulate the IFN-mediated antiviral response[22–24] and RIG-I is a target of NS1 immunosuppressive activity[20,21,25]. Although an immunomodulatory role for 1918 virus NS1 was not shown in mice[8], possibly owing to its species specificity, NS1 does influence the virulence of the H5N1 virus in a mammalian model[5]. This supports the idea that NS1 may be a subject for further investigation as an effector of the aberrations in the macaque immune response to 1918 virus infection and emphasizes the value of development of the macaque model for studying influenza pathogenesis[26].

Results of the present study, the first in nonhuman primates, indicate that atypical expression of the innate immune response may be a critical determinant of the severity and outcome of infection by the 1918 virus. Better understanding of the virus–host interaction will aid development of interventions that can interfere with the virus' ability to modulate host innate immune responses and thus alter outcome of severe infections due to viruses such as the H5N1 viruses circulating at present.

METHODS

Viruses. Genes of the 1918 (GenBank DQ208309, DQ208310, DQ208311, AF117241, AY744935, AF250356, AY130766, AF233238) and K173 virus were constructed with the 5′ and 3′ noncoding sequences of A/WSN/33 (H1N1) and cloned into plasmid vector pPolI, as previously described[3]. The 1918 and K173 viruses were generated by reverse genetics[12], and titred stocks prepared[3], as previously described. All procedures with the 1918 influenza virus were performed in the biosafety level 4 facility of the National Microbiology Laboratory of the Public Health Agency of Canada.

Determination of the lethal dose for the 1918 virus in mice. Isoflurane-anaesthetized 6-week-old female BALB/c mice were intranasally inoculated with 10-fold serial dilutions (five mice per dilution) of virus in 100 μl of phosphate-buffered saline and monitored daily for disease symptoms and survival. The LD_{50} was calculated using the method of Reed and Muench[27].

Viral pathogenicity in nonhuman primates. Ten cynomolgus macaques (*Macaca fascicularis*), 9–19 years old, weighing 3.7–12 kg, were confirmed seronegative against current H1N1 and H3N2 influenza reference viruses by haemagglutination inhibition assay. Animals were infected with K173 ($n = 3$), as a conventional human virus control, and 1918 ($n = 7$) viruses through a combination of intratracheal (4 ml), intranasal (0.5 ml per nostril), intraocular (0.5 ml per eye) and oral (1 ml) routes with suspension containing 10^6 PFU ml^{-1} (infectious dose by all routes is 7×10^6 PFU). Before infection and on days 3, 6 and 8 post-infection, blood and oral, nasal, throat, genital and rectal swabs were collected from anaesthetized animals and suspended in 1 ml of MEM containing 0.3% bovine serum albumin and antibiotics (MEM/BSA). Animals were monitored daily for clinical signs, using an approved scoring sheet, and on days 3, 6 and 8 post-infection vital signs including pulse rate, blood pressure, temperature, respiration rate and blood O_2 saturation, as measured by pulse oximetry, were recorded.

One K173- and two 1918-virus-infected animals were euthanized on day 3 and on day 6 post-infection; all remaining animals were euthanized on day 8 post-infection for complete necropsy. Tissue samples were placed in RNAlater (Ambion) for subsequent RNA extraction (Qiagen RNAlater kit). The remaining tissue was fixed in 10% phosphate-buffered formalin. Fixed tissues were dehydrated, embedded in paraffin, cut into 5-μm-thick sections and stained with standard haematoxylin and eosin. For viral antigen detection, sections were processed for immunostaining by the two-step dextran polymer method (DAKO), with a rabbit polyclonal antibody to WSN.

All animal experiments were performed under an approved animal-use document and according to the guidelines of the Canadian Council on Animal Care.

Expression microarrays. Equal masses of total RNA isolated from bronchi collected from infected macaques were amplified with a Low RNA Input Linear Amplification Kit (5188-5339; Agilent Technology) according to the manufacturer's instructions and as previously described[28]. Global gene expression in infected bronchi was compared to pooled RNA prepared from equal masses of total RNA from whole lung tissue of three uninfected macaques. Mock-infected intact lung was used as a reference for the microarrays because of a lack of mock-infected bronchus tissue. Probe labelling and microarray slide hybridization were performed as previously described[28] with custom rhesus macaque (*Macaca mulatta*) oligonucleotide microarrays containing 22,000 rhesus probes corresponding to ~18,000 unique rhesus genes (designed in collaboration with Agilent Technologies). Raw microarray image files were processed using Feature Extraction 8.1 software (Agilent Technologies) and entered into a custom-designed relational database (Expression Array Manager) and analysed with Rosetta Resolver System 5.1 (Rosetta Biosoftware, Seattle, Washington) and Spotfire Decision Site for Functional Genomics 8.1 (Spotfire, Somerville, Massachusetts). Primary data are available at <http://expression.microslu.washington.edu> in accordance with proposed MIAME standards[29]. Gene ontology analysis was performed using FatiGO (http://fatigo.bioinfo.cipf.es/) as described in reference 30.

Serum cytokine analysis. Serum was obtained from blood collected in K_2EDTA vacutainer tubes (BD Biosciences) that were centrifuged at 1,540*g* for 10 min and γ-irradiated (5 Mrad) for removal from biosafety level 4 containment. Commercial kits for detection of human cytokines and chemokines (IL-2, IL-4, IL-5, IL-6, IFN-γ, TNF-α, IL-8, IL-10, IL-1β, IL12p70, CCL2, CCL5, M1G and IP-10) were screened for cross-reactive detection of homologous macaque proteins. Of these, IL-2, IL-4, IL-6, IL-8, CCL2, TNF-α, IFN-γ and CCL5 exhibited significant cross-reactivity and were detected in supernatants of lipopolysaccharide or phorbol 12-myristate 13-acetate/ionomycin-stimulated macaque peripheral blood mononuclear cells. Levels of each were assayed using the Human Chemokine CBA Kit I and the human IL-6 Flex set (BD Biosciences) according to the manufacturer's instructions. The samples were acquired with the LSRII (BD Biosciences) flow cytometer. Chemokine and IL-6 samples were analysed with BD Biosciences' CBA and FCAP software, respectively.

Virus titration. Tissue homogenates (10% w/v) were prepared in MEM/BSA. Debris was pelleted by centrifugation (2,000*g*, 5 min) and virus titres determined in 10-fold serial dilutions of supernatant by standard plaque assay on MDCK cells, in duplicate for each dilution. Virus was similarly determined in the blood and swab suspensions.

Received 11 September; accepted 29 November 2006.

1. Johnson, N. P. & Mueller, J. Updating the accounts: global mortality of the 1918–1920 "Spanish" influenza pandemic. *Bull. Hist. Med.* **76,** 105–115 (2002).
2. Tumpey, T. M. *et al.* Existing antivirals are effective against influenza viruses with genes from the 1918 pandemic virus. *Proc. Natl Acad. Sci. USA* **99,** 13849–13854 (2002).
3. Kobasa, D. *et al.* Enhanced virulence of influenza A viruses with the haemagglutinin of the 1918 pandemic virus. *Nature* **431,** 703–707 (2004).
4. Tumpey, T. M. *et al.* Characterization of the reconstructed 1918 Spanish influenza pandemic virus. *Science* **310,** 77–80 (2005).
5. Seo, S. H., Hoffmann, E. & Webster, R. G. Lethal H5N1 influenza viruses escape host anti-viral cytokine responses. *Nature Med.* **8,** 950–954 (2002).
6. Reid, A. H., Fanning, T. G., Hultin, J. V. & Taubenberger, J. K. Origin and evolution of the 1918 "Spanish" influenza virus hemagglutinin gene. *Proc. Natl Acad. Sci. USA* **96,** 1651–1656 (1999).
7. Reid, A. H., Fanning, T. G., Janczewski, T. A. & Taubenberger, J. K. Characterization of the 1918 "Spanish" influenza virus neuraminidase gene. *Proc. Natl Acad. Sci. USA* **97,** 6785–6790 (2000).
8. Basler, C. F. *et al.* Sequence of the 1918 pandemic influenza virus nonstructural gene (NS) segment and characterization of recombinant viruses bearing the 1918 NS genes. *Proc. Natl Acad. Sci. USA* **98,** 2746–2751 (2001).
9. Reid, A. H., Fanning, T. G., Janczewski, T. A., McCall, S. & Taubenberger, J. K. Characterization of the 1918 "Spanish" influenza virus matrix gene segment. *J. Virol.* **76,** 10717–10723 (2002).
10. Reid, A. H., Fanning, T. G., Janczewski, T. A., Lourens, R. M. & Taubenberger, J. K. Novel origin of the 1918 pandemic influenza virus nucleoprotein gene. *J. Virol.* **78,** 12462–12470 (2004).
11. Taubenberger, J. K. *et al.* Characterization of the 1918 influenza virus polymerase genes. *Nature* **437,** 889–893 (2005).
12. Neumann, G. *et al.* Generation of influenza A viruses entirely from cloned cDNAs. *Proc. Natl Acad. Sci. USA* **96,** 9345–9350 (1999).

©2007 Nature Publishing Group

13. Rimmelzwaan, G. F. *et al.* Pathogenesis of influenza A (H5N1) virus infection in a primate model. *J. Virol.* **75,** 6687–6691 (2001).
14. Kuiken, T., Rimmelzwaan, G. F., Van Amerongen, G. & Osterhaus, A. D. Pathology of human influenza A (H5N1) virus infection in cynomolgus macaques (*Macaca fascicularis*). *Vet. Pathol.* **40,** 304–310 (2003).
15. Winternitz, M. C., Wason, I. M. & McNamara, F. P. *The Pathology of Influenza.* (Yale Univ. Press, New Haven, Connecticut, 1920).
16. Hayden, F. G. *et al.* Local and systemic cytokine responses during experimental human influenza A virus infection. Relation to symptom formation and host defense. *J. Clin. Invest.* **101,** 643–649 (1998).
17. Skoner, D. P., Gentile, D. A., Patel, A. & Doyle, W. J. Evidence for cytokine mediation of disease expression in adults experimentally infected with influenza A virus. *J. Infect. Dis.* **180,** 10–14 (1999).
18. Kash, J. C. *et al.* Genomic analysis of increased host immune and cell death responses induced by 1918 influenza virus. *Nature* **443,** 578–581 (2006).
19. de Jong, M. D. *et al.* Fatal outcome of human influenza A (H5N1) is associated with high viral load and hypercytokinemia. *Nature Med.* **12,** 1203–1207 (2006).
20. Matikainen, S. *et al.* Tumor necrosis factor alpha enhances influenza A virus-induced expression of antiviral cytokines by activating RIG-I gene expression. *J. Virol.* **80,** 3515–3522 (2006).
21. Kato, H. *et al.* Differential roles of MDA5 and RIG-I helicases in the recognition of RNA viruses. *Nature* **441,** 101–105 (2006).
22. Garcia-Sastre, A. *et al.* Influenza A virus lacking the NS1 gene replicates in interferon-deficient systems. *Virology* **252,** 324–330 (1998).
23. Krug, R. M., Yuan, W., Noah, D. L. & Latham, A. G. Intracellular warfare between human influenza viruses and human cells: the roles of the viral NS1 protein. *Virology* **309,** 181–189 (2003).
24. Li, S., Min, J. Y., Krug, R. M. & Sen, G. C. Binding of the influenza A virus NS1 protein to PKR mediates the inhibition of its activation by either PACT or double-stranded RNA. *Virology* **349,** 13–21 (2006).
25. Pichlmair, A. *et al.* RIG-I-mediated antiviral responses to single-stranded RNA bearing 5′ phosphates. *Science* **314,** 997–1001 (2006).
26. Baas, T. *et al.* Integrated molecular signature of disease: analysis of influenza virus-infected macaques through functional genomics and proteomics. *J. Virol.* **80,** 10813–10828 (2006).
27. Reed, L. J. & Muench, H. A simple method of estimating fifty per cent endpoints. *Am. J. Hyg.* **27,** 493–497 (1938).
28. Kash, J. C. *et al.* Global suppression of the host antiviral response by Ebola- and Marburgviruses: increased antagonism of the type I interferon response is associated with enhanced virulence. *J. Virol.* **80,** 3009–3020 (2006).
29. Brazma, A. *et al.* Minimum information about a microarray experiment (MIAME)—toward standards for microarray data. *Nature Genet.* **29,** 365–371 (2001).
30. Al-Shahrour, F., Minguez, P., Vaquerizas, J. M., Conde, L. & Dopazo, J. BABELOMICS: a suite of web tools for functional annotation and analysis of groups of genes in high-throughput experiments. *Nucleic Acids Res.* **33,** W460–W464 (2005).

Supplementary Information is linked to the online version of the paper at www.nature.com/nature.

Acknowledgements We thank D. Dick, J. Gren, A. Grolla and P. Melito for help with animal care, and V. Carter, M. Thomas and S. Proll for microarray technical assistance. We also thank J. Gilbert for editing the manuscript. This work was supported by the Public Health Agency of Canada (D.K., S.M.J. and H.F.), by grants-in-aid for scientific research on priority areas from the Ministries of Education, Culture, Sports, Science, and Technology, Japan (Y.K. and K.S.), by CREST (Japan Science and Technology Agency; Y.K.), and by private grants to Y.K.

Author Information Microarray data were deposited at Arrayexpress with accession number E-TABM-181. Reprints and permissions information is available at www.nature.com/reprints. The authors declare no competing financial interests. Correspondence and requests for materials should be addressed to Y.K. (kawaokay@svm.vetmed.wisc.edu).

©2007 Nature Publishing Group